Open access • Journal Article • DOI:10.1103/PHYSREVB.86.245434

Potential energy surface for graphene on graphene: Ab initio derivation, analytical description, and microscopic interpretation — Source link

Marco Reguzzoni, Annalisa Fasolino, Elisa Molinari, Maria Clelia Righi

Institutions: Radboud University Nijmegen

Published on: 27 Dec 2012 - Physical Review B (American Physical Society)

Topics: Elementary charge, Graphene and Potential energy surface

Potential energy surface for graphene on graphene: *Ab initio* derivation, analytical description, and microscopic interpretation

M. Reguzzoni,[1,2] A. Fasolino,[3] E. Molinari,[1,2] and M. C. Righi[1,2,*]

[1]*CNR Institute of Nanoscience, S3 Center, Via Campi 213/A, I-41125 Modena, Italy*

[2]*Dipartimento di Fisica, Università di Modena e Reggio Emilia, Via Campi 213/A, I-41125 Modena, Italy*

[3]*Institute for Molecules and Materials, Radboud University Nijmegen, Heyendaalseweg 135, NL-6525 AJ Nijmegen, The Netherlands*

(Received 19 October 2012; published 27 December 2012)

We derive an analytical expression that describes the interaction energy between two graphene layers identically oriented as a function of the relative lateral and vertical positions, in excellent agreement with first principles calculations. Thanks to its formal simplicity, the proposed model allows for an immediate interpretation of the interactions, in particular of the potential corrugation. This last quantity plays a crucial role in determining the intrinsic resistance to interlayer sliding and its increase upon compression influences the frictional behavior under load. We show that, for these weakly adherent layers, the corrugation possesses the same nature and z dependence of Pauli repulsion. We investigate the microscopic origin of these phenomena by analyzing the electronic charge distribution: We observe a pressure-induced charge transfer from the interlayer region toward the near-layer regions, with a much more consistent depletion of charge occurring for the AA stacking than for the AB stacking of the two layers.

DOI: 10.1103/PhysRevB.86.245434 PACS number(s): 34.20.Gj, 68.65.Pq, 71.15.Mb

I. INTRODUCTION

There is an increasing interest in the physics and application of few layer graphene (FLG) films. A wide set of applications, such as the use of FLG for nanoelectromechanical systems and for lubrication, involve the relative displacement of the layers composing the film. The effects of shear forces constitute, thus, an important aspect of FLG physics, which has been recently investigated by different experiments.[1–9] Moreover, it has been demonstrated that the electronic properties in FLG can be tuned by changing the layer stacking. A spontaneous gap opening has been detected in three layer graphene (3LG) when passing from Bernal (ABA) to rhombohedral (ABC) stacking.[10] The important implications of this finding for a possible use of graphene in electronic devices have stimulated recent experimental studies on the horizontal shifting of graphene layers.[11]

At the fundamental level, the mobility of one graphene layer onto another is governed by the shape of the potential energy surface (PES), which describes the interlayer interaction as a function of the relative position of two layers. In particular, the PES corrugation determines the intrinsic resistance to sliding[12] and the maximum energy that can be dissipated by frictional mechanisms. The potential corrugation and hence the frictional force typically increase when the interlayer spacing is reduced by imposing an external load.

Many efforts have been dedicated towards the understanding of the interlayer binding in graphite[13–23] and its dependence on the layer stacking.[24–27] Here we consider some of the most widely used numerical methods to describe graphite/FLG and compare their description of the potential corrugation. We focus on bilayer graphene since the corrugation of the interlayer potential is mainly determined by nearest-neighbor interlayer interactions. We apply a procedure to parametrize the PES that we have developed for rare gas adsorbed on metals,[28,29] and show that an excellent fitting of the density functional theory (DFT) data for bilayer graphene can be obtained by describing the PES as a three-dimensional function, which is a sum of a repulsive contribution of Pauli nature and an attractive contribution of van der Waals (vdW) nature. Beside being formally simple, the derived analytical expression allows for a direct interpretation of the physical interactions, in particular of the potential corrugation. We provide a physical rationale for the derived z dependence of the potential corrugation by analyzing the electronic charge displacements occurring upon bilayer compression.

In Sec. II we show the results of first-principles and empirical calculations for the interlayer energy as a function of the relative lateral and vertical positions of two graphene layers. In Sec. III we describe the procedure to parametrize the PES and validate it against first principles results. In Sec. IV we analyze the microscopic origin of the potential corrugation.

II. SAMPLING THE PES BY DIFFERENT NUMERICAL METHODS

We calculate the interaction energy for different relative positions of two graphene layers, obtaining in this way a sampling of the PES. For these calculations we use different DFT-based and empirical methods for the purpose of comparison, in particular on the ability to describe the potential corrugation. We firstly performed standard DFT calculations with the exchange correlation functional described by local density approximation (LDA). Then, we took into account the vdW interactions both by semi-empirical inclusion, as in the DFT-D method proposed by Grimme,[30] and by an explicit nonlocal functional of the density, as in the vdW density functional (vdW-DF) methods.[31]

In the semi-empirical approach, the total energy of the system is $E_{\mathrm{tot}} = E_{\mathrm{PBE}} + E_{\mathrm{vdW}}$, where E_{PBE} is the DFT-GGA total energy calculated with the Perdew Burke Ernzerhof (PBE) parametrization[32] of the exchange correlation functional and E_{vdW} is the total energy given by the sum of $-C_6/r_{ij}^6$ interactions occurring between each pair of nuclei. Each contribution is multiplied by a damping function that controls

the strength of the dispersion correction by means of a scaling factor and cuts it off at short interatomic separations. We use a scaling factor $s_6 = 0.65$, C_6 coefficients, and vdW radii for the carbon atoms given by Grimme.[30] Pairwise interactions are summed within a radius of 200 a.u.

In the vdW-DF method,[31] the energy functional is written as $E_{\rm tot} = E_0 + E_c^{nl}$, where E_0 is obtained from the DFT-revPBE[33] energy and E_c^{nl} describes the nonlocal part of the correlation energy, according to the analytical expression given in Ref. 31. We performed plane-wave/pseudopotential calculations.[34] On the basis of test calculations for bulk graphite, we adopted a kinetic energy cutoff $E_{\rm cut} = 60$ Ry for wave functions, and $4E_{\rm cut}$ for charge density. In calculations where the ionic species are described by ultrasoft pseudopotentials, we use $6E_{\rm cut}$ for the charge density cutoff. We use a hexagonal cell with (1×1) in-plane size and vertical axis 32 Å long. The **k**-point sampling of the Brillouin zone is realized with a $12 \times 12 \times 1$ Monkhorst-Pack grid.[35]

In classical molecular dynamics (MD) simulations,[36] we describe the intralayer interaction by the REBO potential[37,38] and the interlayer interaction either by the Lennard-Jones (LJ) potential or by the Kolmogorov-Crespi (KC) potential.[24] We use the parameters $\sigma = 3.41$ Å and $\epsilon = 2.39$ meV for the LJ potential, as in Ref. 39, and the same parameters of the original paper for the KC potential.[24] A cutoff of 14 Å and a two-dimensional cell containing 112 atoms per layer are used for both kinds of interlayer interactions.

The interlayer interaction between two layers in AB stacking is reported as a function of the separation in Fig. 1(a) for all the considered methods. It is calculated as $e = \frac{1}{2}(E_{12} - 2E_1)$, where E_{12} is the total energy of the system containing the two interacting layers and E_1 is the total energy of an isolated graphene layer.

We can see that DFT-LDA underestimates the depth of the minimum. A problem which is solved by the inclusion of the vdW interactions as in the DFT-D and vdW-DF schemes. We notice that vdW-DF produces a deeper minimum and higher equilibrium distance than DFT-D. The present vdW-DF curve is similar to that previously published in Ref. 44, where a minimum of 45.5 meV is obtained for $z = 3.6$ Å. The two empirical methods (REBO + LJ and REBO + KC) show almost the same trend as DFT-D, with a small deviation at short range.

We then calculate the interaction energy for the relative lateral positions of the two layers indicated in the inset of Fig. 1(b) (each point indicates the position of the origin of the unit cell of the upper layer, not shown, within the unit cell of the lower layer, represented by arrows). The distance between the two layers is optimized at each location to its equilibrium value $z_{\rm eq}$. The energy values reported in Fig. 1(b) are referred to the minimum, which is obtained for the AB stacking of the two layers. The highest maximum corresponds to the AA stacking and the lower one to the PES saddle point. The atomic configurations competing with these sites are described in the following. The numerical values obtained for all the considered methods are summarized in Table I.

The binding energy for AB stacking $e_{\rm min}$ and the corresponding equilibrium interlayer distance $z_{\rm eq}$ are slightly higher than those we obtained for graphite.[45] The results are consistent with the available experimental data, except for DFT-LDA, which largely underestimates the binding energy,

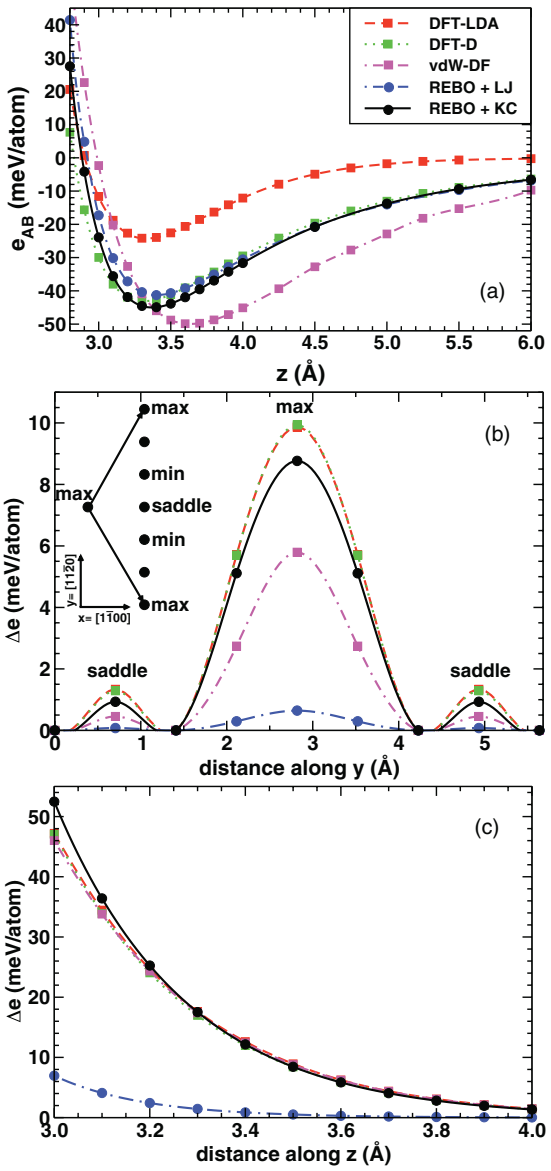

FIG. 1. (Color online) Interaction energy per atom of two graphene layers obtained by different numerical methods. The lines are guides for the eyes. In (a) the relative lateral position of the two layers corresponds to the AB stacking. In (b) the considered lateral positions are represented in the hexagonal unit cell, shown in the inset, the layer separation is optimized at each location. The reported values are referred to the energy minimum. In (c) the difference $\Delta e^{\rm max} = e_{AA} - e_{AB}$ is reported as a function of the interlayer separation z.

even if the equilibrium interlayer distance is not too far from the experimental value.

In the third column of Table I we report the maximum difference obtained for the equilibrium distances: $\Delta z_{\rm max} = z_{\rm eq}^{AA} - z_{\rm eq}^{AB}$. The lateral variation of the interlayer interaction gives rise to a lateral dependence not only of the binding energy, but also of the equilibrium interlayer distance. This quantity in some systems, as, for example, rare gases monolayers adsorbed on metals, can be directly measured. We are not aware of any experimental evaluation for graphene, however, the corrugation of the interlayer distance is predicted both

TABLE I. The minimum values of the interaction energy e_{min} and equilibrium distance z_{eq} are obtained for the AB stacking of two graphene layers. The larger increases of these quantities, Δz_{max} and Δe_{max}, are obtained for the AA stacking. The height of the PES saddle points Δe_{saddle} is reported in the last column. Distances are reported in Å and energies in meV/atom.

	z_{eq}	e_{min}	Δz_{max}	Δe_{max}	Δe_{saddle}
DFT-LDA	3.33	−24.2	0.27	9.9	1.3
DFT-D	3.31	−43.1	0.26	9.9	1.3
vdW-DF	3.62	−49.9	0.02	5.8	0.5
REBO + LJ	3.39	−41.3	0.01	0.6	0.1
REBO + KC	3.37	−45.0	0.23	8.9	1.4
Exp. graphite	3.34[a]	43[b], 35^{+15}_{-10}[c], 52 ±5[d]	-	-	-

[a]Reference 40,
[b]Reference 41,
[c]Reference 42,
[d]Reference 43

by the DFT-LDA and DFT-D calculations. On the contrary, vdW-DF does not capture this variation and Δz_{max} is close to zero in this case (Table I).

In the last two columns of Table I we report the PES corrugation at the maxima and saddle points. We can observe that the DFT-LDA and DFT-D methods provide the same description of the PES corrugation [see also Fig. 1(b)]. Our results, thus, confirm the observation of the authors of Ref. 24 that the vdW contribution, while essential to obtain the correct interlayer binding, does not significantly affect the potential corrugation. The PES corrugation calculated with vdW-DF is lower than those predicted by the other two DFT methods, in particular, $\Delta e^{vdW-DF}_{saddle}$ is almost negligible. Our DFT-LDA and DFT-D results for Δe_{max} are in agreement with that obtained for bulk graphite by the adiabatic-connection fluctuation-dissipation theorem in the random phase approximation (ACFDT-RPA): the AB stacking turned out to be energetically more favorable than the AA stacking by 10 meV/atom.[15] Within LDA Kolmogorov and Crespi obtained $\Delta e_{max} = 15$ meV/atom,[24] whereas Charlier *et al.* found $\Delta e_{max} = 17$ meV/atom.[13] In these calculations the interlayer distance was fixed to the equilibrium value obtained for the AB stacking, without recalculating it for the AA stacking. This produces an overestimation of the potential corrugation. The same reason can explain the difference between our results and those obtained by Lebedeva *et al.*, who found $\Delta e^{DFT-D}_{max} = 19.5$ meV/atom and $\Delta e^{vdW-DF}_{max} = 18.9$ meV/atom for a fixed interlayer distance of 3.25 Å.[26]

In Fig. 1(c) we report the maximum potential corrugation as a function of the interlayer distance, $\Delta e_{max}(z)$. The behavior of the corrugation at distances lower than the equilibrium one has a high impact on the frictional properties of a system when an external load is applied. Thus, it is important that the empirical potentials adopted in MD simulations of graphene friction provide a good description of $\Delta e(z)$. We can observe that while the REBO + KC potential describes the corrugation in agreement with the DFT-based results, the REBO + LJ potential produces a potential corrugation which is almost negligible at normal load and increases extremely slowly by decreasing the interlayer separation. Therefore the use of the LJ potential to describe interlayer interactions in simulations of graphene friction is a questionable choice.

III. PARAMETRIZATION OF THE PES

To parametrize the PES for bilayer graphene we adopt the DFT-D data as benchmark. However, the procedure here described can be applied to fit the data obtained by other, even more sophisticated methods. Among the DFT-based methods including the dispersion that we have considered, the DFT-D one seems the most suitable to obtain an accurate description of the PES. This method, in fact, gives the maximum potential corrugation Δe_{max}, in good agreement with the superior ACFDT-RPA method[15] and, unlike vdW-DF, is able to capture the corrugation of the interlayer distance Δz.

To construct the PES we firstly fit the DFT-D interaction energies as a function of z with the analytical expression

$$V(z) = C_0 e^{-zC_1} - \frac{C_2}{z^4}, \tag{1}$$

which is a sum of two contributions: The positive one describes the Pauli repulsion at short distances, the negative one the

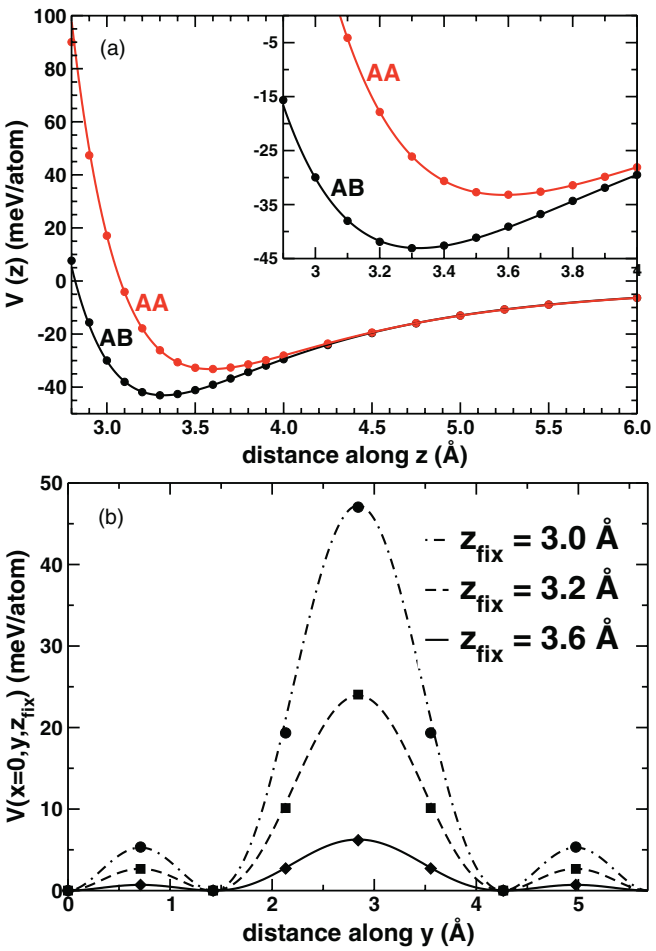

FIG. 2. (Color online) Comparison of the results obtained by the parametric function of Eq. (4) (continuous lines) with DFT-D calculations (circles). In (a) the interaction energy of two graphene layers as a function of separation. In (b) the PES profile along the armchair direction for different values of the vertical separation.

TABLE II. Numerical values of the parameters appearing in Eq. (1), which describes the interaction energy between two layers as a function of the separation z. Two different terns of parameters are obtained by considering the AA and the AB stacking of the two layers.

	C_0 (10^6 meV)	C_1 (Å^{-1})	C_2 (meVÅ^4)
max (AA)	2.75075	3.349208	8258.11
min (AB)	1.63093	3.347616	8184.70

long-range attraction. For the repulsive term we choose an exponential decay that mimics the decay of the surface charge density into the vacuum, while for the attractive term we use a power law z^{-n} with $n = 4$, obtaining an excellent fitting of the DFT-D data in the range 3.0–6.0 Å, as can be seen in Fig. 2(a). Spanu *et al.*[14] found $n = 4.2$ by fitting the results obtained by quantum Monte Carlo in the range 3–9 Å. By fitting the ACFDT-RPA correlation energy Lebegue *et al.*[15] suggested that the exponent might drop to values around 3 at larger distances, as expected from the analytical quantum-mechanical calculation of the dipole-image dipole interactions.[46]

Since the relative strength of the attractive and the repulsive contributions of the interaction varies by changing the relative lateral position of the two layers, we repeat the fitting procedure for the AB and AA stacking [Fig. 2(a)] obtaining the two terns of the parameters reported in Table II.

Since the parameter variation along the surface presents the symmetry of the underlying lattice, we describe each parameter C_i as a periodic function

$$C_i(x,y) = C_i^{\max} - \Delta_i u(x,y), \quad i = 0,1,2, \tag{2}$$

where $\Delta_i = C_i^{\max} - C_i^{\min}$ measures the amplitude for the ith parameter swing between the AA and AB stacking and $u(x,y) = \delta[3 - \sum_{\mathbf{g}} \cos(\mathbf{g}\cdot\mathbf{r})]$, the sum runs over the first three reciprocal $\mathbf{g}$ vectors of the hexagonal lattice ($\mathbf{g}_{10}$,$\mathbf{g}_{01}$,$\mathbf{g}_{11}$)

$$\sum_{\mathbf{g}} \cos(\mathbf{g}\cdot\mathbf{r}) = 2\cos\theta_x \cos\theta_y + \cos 2\theta_y,$$
$$\theta_x = \frac{2\pi x}{a}; \quad \theta_y = \frac{2\pi y}{a\sqrt{3}}. \tag{3}$$

The factor $\delta = \frac{2}{9}$ is used to normalize the amplitude of $u(x,y)$ to 1 (Ref. 47).

We arrived in this way at the definition of a three-dimensional function

$$V(x,y,z) = C_0(x,y)e^{-zC_1(x,y)} - \frac{C_2(x,y)}{z^4}, \tag{4}$$

which analytically describes the interaction energy between two graphene layers identically oriented as a function of their relative position. As can be seen in Fig. 2(b), where V is plotted along the armchair direction for different values of the separation, the agreement with DFT-D data is excellent. This holds not only for the energies, but also for the forces: The forces obtained by analytical derivation reproduce very well the Hellmann-Feynman forces of self-consistent DFT-D calculations.

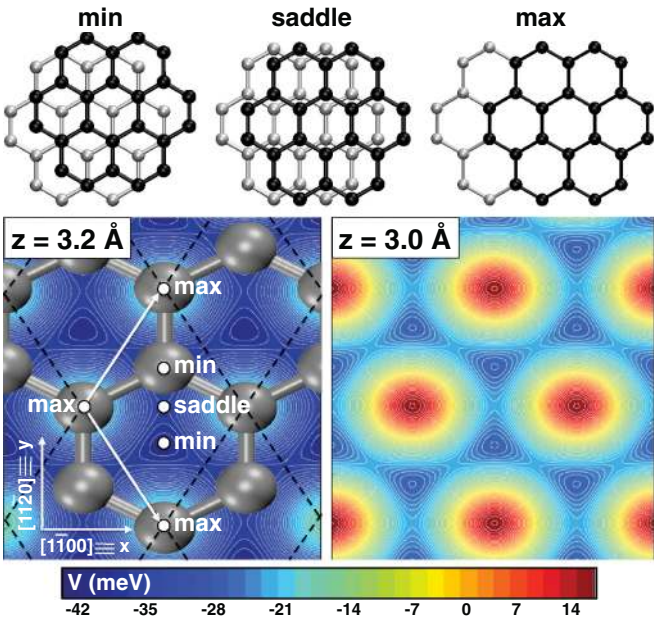

FIG. 3. (Color online) The function $V(x,y,z)$ [Eq. (4)], which describes the PES for bilayer graphene, is represented in two dimensions for two different values of the interlayer separation z. The bilayer configurations corresponding to the PES stationary points are represented in the top part of the picture.

IV. ANALYSIS OF THE POTENTIAL CORRUGATION

A two-dimensional representation of $V(x,y,z)$ is reported in Fig. 3. The stacking configurations corresponding to the PES stationary points are schematically represented in the same picture. They can be obtained by shifting the unit cell origin of the superimposed layer (not shown in Fig. 3) along the y axis. The PES maximum corresponds to the AA stacking with all the carbon atoms of the upper layer on top of those of the lower ones; the PES minimum corresponds to AB stacking with half of the atoms on top, the other half at the hollow sites directly above the centers of the hexagonal rings; the saddle stacking presents two connected carbon atoms falling within every hexagonal ring. Scanning tunneling microscope (STM) images corresponding to the saddle configuration has been acquired during the tip-induced horizontal shift of the top layer in a graphite sample.[11,48] In agreement with our findings, this observation indicates that the saddle configuration (defined as the "no overlap" configuration by the authors of Ref. 11) is the configuration the top layer goes through in passing from one PES minima to another (i.e., from ABA to ABC stacking on graphite). Upon bilayer compression, the location of the PES stationary points might change,[29] this is not the case for bilayer graphene: As can be seen in Fig. 3, the PES shape at the two selected nonequilibrium distances is the same, apart from the enhanced corrugation at the lower separation. Pressure-induced modifications to the in-plane lattice parameter are negligible.

The z dependence of the potential corrugation at the PES maxima and saddle points is shown Fig. 4, where DFT-D data are also reported for comparison. In the zoomed-in part of the graph, the contributions to the corrugation at AA arising from the repulsive and the attractive parts of the potential are represented separately. It appears evident that the corrugation

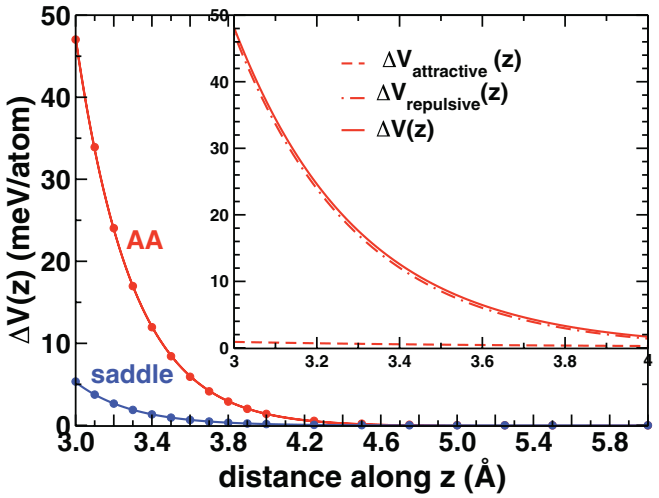

FIG. 4. (Color online) PES corrugations at the maxima and saddle points as a function of distance derived analytically (continuous lines) and by DFT-D (circles). The inset shows the contributions at the AA corrugation arising from the repulsive and attractive parts of the potential.

is almost completely determined by the difference in the repulsive energy while the long-range attraction produces a negligible corrugation. This definitely demonstrates that the adhesion due to interactions of vdW nature does not produce significant effects on the potential corrugation and, thus, on the intrinsic resistance to the sliding of the system. Frictional forces at fully saturated interfaces are almost completely determined by the Pauli repulsion existing between the two surfaces, which varies as a function of their relative alignment. By neglecting the part of the corrugation arising from the attractive part of the potential and assuming $\Delta_1 \simeq 0$, it is possible to derive a simplified expression for $\Delta V(x,y,z)$

$$\Delta V(x,y,z) \simeq V_R^{\min}(z)\zeta(x,y), \quad \text{with} \quad \zeta(x,y) = \frac{C_0(x,y) - C_0^{\min}}{C_0^{\min}}. \tag{5}$$

The potential corrugation at a given (x,y) site is approximated as the repulsive part of the potential at the AB site $V_R^{\min}(z) = C_0^{\min} e^{-zC_1^{\min}}$ multiplied by a factor $\zeta(x,y)$ that measures the strength of the repulsive coefficient $C_0(x,y)$ at the selected site with respect to the AB site. This suggests that, apart from a scaling factor, the corrugation increases upon the bilayer compression in the same way as the short-range repulsion increases. The ζ factor for the AA stacking is $\zeta_{\max} = 0.687$ and for the saddle $\zeta_{\text{saddle}} = 0.076$ about nine times lower because of the difference in the Pauli repulsion at these two sites.

To understand the microscopic origin of the differences in the repulsive character of the different bilayer configurations, we analyze their electronic charge distributions. In Fig. 5(a) we show the changes in the electronic charge occurring when a compressed bilayer is formed from two isolated layers [i.e., we plot $\Delta\rho = \rho_{12} - (\rho_1 + \rho_2)$, where ρ_{12} is the charge density of the bilayer with $z = 3$ Å interlayer spacing, and ρ_1 and ρ_2 are the charge densities of single graphene layers at $z = 0$ Å and $z = 3$ Å, respectively]. In Fig. 5(a) a slice of $\Delta\rho$ is

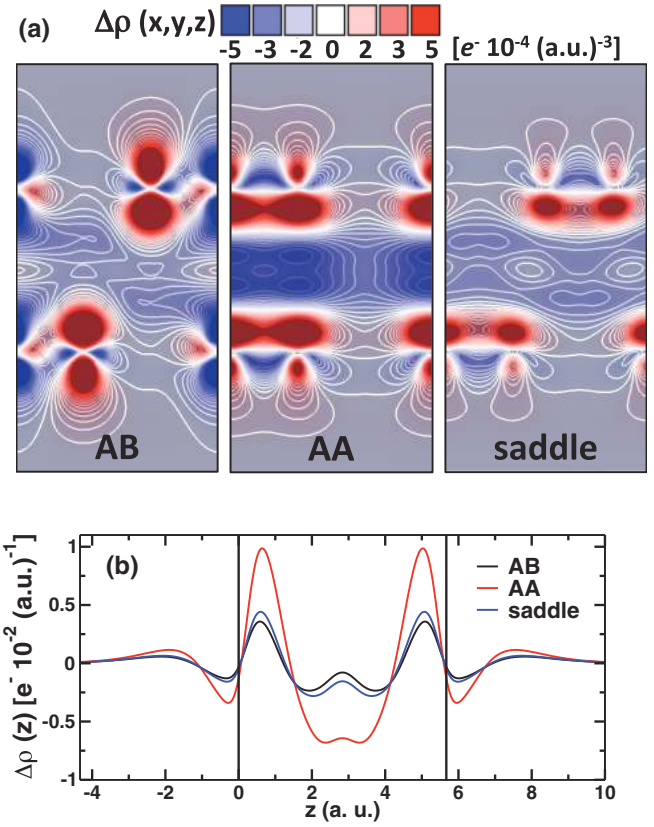

FIG. 5. (Color online) Changes in the electronic charge distribution of a compressed bilayer $z = 3.0$ Å, with respect to the sum of the charge distributions of two isolated layers. (a) The same scale is used for different stacking configurations to highlight the differences. (b) The profile of $\Delta\rho$ along the z direction is obtained by two-dimensional integration.

taken in the yz plane with origin (0,0,0). It can be seen that the bilayer compression induces a charge depletion from the region in between the two layers. This charge depletion is much more consistent in the AA than in the AB and saddle configurations. The depleted electronic charge gathers in the regions around the nuclei, where the electrostatic potential is lower, with a consequent increase of Pauli repulsion. As previously noted for graphite at equilibrium,[25] we observe that in the AB configuration the charge gathers around "hollow" carbon atoms only, while "on-top" carbon atoms are depleted. In Fig. 5(b) the profile of the charge displacement along the z direction, obtained by integration in two dimensions, clearly reveals the presence of charge accumulation in the proximity of each layer (indicated by a vertical line) and charge depletion in the middle. The depths of $\Delta\rho(z)$ in the depleted region for the AA and saddle stackings differ by a factor of 9. This suggests that the different behavior of the electronic charge distribution upon bilayer compression is what determines the corrugation increase, which is more enhanced for the AA than the *saddle* stacking. The "acceptor-like" electronic character of the intralayer regions compared to the "donor-like" character of the interlayer region may be tuned by the chemical modifications of graphene by the presence of a substrate. In particular, substrates with different electronic affinities may cause $\Delta V(z)$ to deviate from the curves of Fig. 4 and, thus, change friction for interlayer sliding.

V. SUMMARY AND CONCLUSION

A comparison is made on the ability of different DFT and empirical methods to describe the binding energy of bilayer graphene and in particular its variations as a function of the relative lateral position of the two layers (i.e., the potential corrugation). The potential corrugation is particularly important for frictional studies since it determines the intrinsic resistance to interlayer sliding and direct experimental evaluations are not available to our knowledge. We found that the inclusion of the vdW interactions in the DFT calculations, both in the semi-empirical DFT-D method proposed by Grimme[30] and by explicit calculation of the nonlocal part of the correlation (vdW-DF method),[31] improves the DFT-LDA description of the binding energy, but leaves unchanged the potential corrugation. In particular, we found that the lateral modulation of the binding energy is described in the same way by DFT-D and DFT-LDA, the largest value of 9.9 meV is obtained for the AA stacking, in agreement with the energy difference between simple hexagonal and Bernal graphite calculated by ACFDT-RPA.[15] The corrugation obtained by vdW-DF is 40% lower. The corrugation of the potential is accompanied by a corrugation of the interlayer equilibrium distance, which according to DFT-D and DFT-LDA has 0.26–0.27 Å maximum amplitude. We also calculate the z dependence of the potential corrugation $\Delta V(z)$, which contains relevant information to understand the friction increase in the presence of an applied load. We noticed that the empirical REBO + KC potential correctly reproduces the results obtained by DFT methods, while the REBO + LJ produces a negligible value of ΔV and fails in describing its z dependence.

On the basis of the above described comparison, we assumed the DFT-D data as a benchmark to derive a parametric function to describe the PES for bilayer graphene, however, the proposed procedure can be applied to fit data obtained by more sophisticated methods or even by experiments. We described the potential well as a sum of repulsive term of Pauli nature, $V_R(z) = C_1 \exp(-zC_2)$, and an attractive term of vdW nature $V_A(z) = C_3 z^{-4}$. The relative strength of the attractive and repulsive interactions varies according to the relative lateral position of the two layers, giving rise to a lateral dependence of the well minimum and of the well depth. We described this variation by including a lateral dependence into the C_i coefficients, which were expanded in Fourier series. The three-dimensional function $V(x,y,z)$ constructed in this way turned out to be in excellent agreement with the DFT-D data. Also the forces obtained by analytical derivation of V reproduce very well the Hellmann-Feynman forces of self-consistent calculations.

Beside the merit of being formally simple, the proposed analytical description of the PES allows for an immediate physical rationale of the interactions, in particular of the potential corrugation. We showed, in fact, that the corrugation due to the long-range attraction is negligible $\Delta V_A \simeq 0$ and the corrugation can be approximated as a site-dependent fraction of the Pauli repulsion: $\Delta V(x,y,z) \simeq \Delta V_R(x,y,z) \simeq \zeta(x,y) V_R^{AB}(z)$. This simple relation shows that in this fully saturated interface the corrugation has the same nature and possesses the same z dependence of Pauli repulsion.

We investigated the microscopic origin of the increase of the potential corrugation upon bilayer compression by analyzing the changes occurring in the electronic charge distributions when the interlayer distance is reduced below the equilibrium value. We observed a pressure-induced charge transfer from the interlayer region toward the near-layer regions, with a much more consistent depletion of charge occurring for the AA stacking than for the AB and the *saddle* stackings. This finding suggests that the corrugation and therefore the resistance to sliding could be tuned by modifying the "donor-like" ("acceptor-like") characters of the interlayer (intralayer) regions, as, for example, by chemical modifications of graphene or by the presence of a substrate with selected electronic affinity.

*mcrighi@unimore.it

[1] K.-S. Kim, H.-J. Lee, C. Lee, S.-K. Lee, H. Jang, J.-H. Ahn, J.-H. Kim, and H.-J. Lee, ACS Nano **5**, 5107 (2011).

[2] T. Filleter, J. L. McChesney, A. Bostwick, E. Rotenberg, K. V. Emtsev, T. Seyller, K. Horn, and R. Bennewitz, Phys. Rev. Lett. **102**, 086102 (2009).

[3] C. Lee, Q. Li, W. Kalb, X.-Z. Liu, H. Berger, R. W. Carpick, and J. Hone, Science **328**, 76 (2010).

[4] Y. J. Shin, R. Stromberg, R. Nay, H. Huang, A. T. Wee, H. Yang, and C. S. Bhatia, Carbon **49**, 4070 (2011).

[5] P. H. Tan, W. P. Han, W. J. Zhao, Z. H. Wu, K. Chang, H. Wang, Y. F. Wang, N. Bonini, N. Marzari, N. Pugno, G. Savini, A. Lombardo, and A. C. Ferrari, Nat. Mater. **11**, 294 (2012).

[6] X. Liu, T. H. Metcalf, J. T. Robinson, B. H. Houston, and F. Scarpa, Nano Lett. **12**, 1013 (2012).

[7] A. P. M. Barboza, H. Chacham, C. K. Oliveira, T. F. D. Fernandes, E. H. M. Ferreira, B. S. Archanjo, R. J. C. Batista, A. B. de Oliveira, and B. R. A. Neves, Nano Lett. **12**, 2313 (2012).

[8] Z. Liu, J. Yang, F. Grey, J. Z. Liu, Y. Liu, Y. Wang, Y. Yang, Y. Cheng, and Q. Zheng, Phys. Rev. Lett. **108**, 205503 (2012).

[9] Z. Liu, J. Z. Liu, Y. Cheng, Z. Li, L. Wang, and Q. Zheng, Phys. Rev. B **85**, 205418 (2012).

[10] W. Bao, L. Jing, J. Velasco, Y. Lee, G. Liu, D. Tran, B. Standley, M. Aykol, S. B. Cronin, and D. Smirnov, Nat. Phys. **7**, 948 (2011).

[11] P. Xu, Y. Yang, D. Qi, S. D. Barber, M. L. Ackerman, J. K. Schoelz, T. B. Bothwell, S. Barraza-Lopez, L. Bellaiche, and P. M. Thibado, Appl. Phys. Lett. **100**, 201601 (2012).

[12] G. Zilibotti and M. C. Righi, Langmuir **27**, 6862 (2011).

[13] J. C. Charlier, X. Gonze, and J. Michenaud, Carbon **32**, 289 (1994).

[14] L. Spanu, S. Sorella, and G. Galli, Phys. Rev. Lett. **103**, 196401 (2009).

[15] S. Lebègue, J. Harl, T. Gould, J. G. Ángyán, G. Kresse, and J. F. Dobson, Phys. Rev. Lett. **105**, 196401 (2010).

[16] D. C. Langreth, B. I. Lundqvist, S. D. Chakarova-Käck, V. R. Cooper, M. Dion, P. Hyldgaard, A. Kelkkanen, J. Kleis, L. Kong, S. Li, P. G. Moses, E. Murray, A. Puzder, H. Rydberg, E. Schröder, and T. Thonhauser, J. Phys.: Condens. Matter **21**, 084203 (2009).

[17] H. Rydberg, M. Dion, N. Jacobson, E. Schröder, P. Hyldgaard, S. I. Simak, D. C. Langreth, and B. I. Lundqvist, Phys. Rev. Lett. **91**, 126402 (2003).

[18]M. Hasegawa and K. Nishidate, Phys. Rev. B **70**, 205431 (2004).
[19]M. Hasegawa, K. Nishidate, and H. Iyetomi, Phys. Rev. B **76**, 115424 (2007).
[20]J. Björk, F. Hanke, C.-A. Palma, P. Samori, M. Cecchini, and M. Persson, J. Phys. Chem. Lett. **1**, 3407 (2010).
[21]O. Hod, J. Chem. Theo. Comput. **8**, 1360 (2012).
[22]F. Ortmann, F. Bechstedt, and W. G. Schmidt, Phys. Rev. B **73**, 205101 (2006).
[23]E. Ziambaras, J. Kleis, E. Schröder, and P. Hyldgaard, Phys. Rev. B **76**, 155425 (2007).
[24]A. N. Kolmogorov and V. H. Crespi, Phys. Rev. B **71**, 235415 (2005).
[25]J. Charlier, X. Gonze, and J. Michenaud, Europhys. Lett. **28**, 403 (1994).
[26]I. V. Lebedeva, A. A. Knizhnik, A. M. Popov, Y. E. Lozovik, and B. V. Potapkin, Phys. Chem. Chem. Phys. **13**, 5687 (2011).
[27]G. Savini, Y. Dappe, S. Öberg, J.-C. Charlier, M. Katsnelson, and A. Fasolino, Carbon **49**, 62 (2011).
[28]M. C. Righi and M. Ferrario, J. Phys.: Condens. Matter **19**, 305008 (2007).
[29]M. C. Righi and M. Ferrario, Phys. Rev. Lett. **99**, 176101 (2007).
[30]S. Grimme, J. Comput. Chem. **27**, 1787 (2006).
[31]M. Dion, H. Rydberg, E. Schröder, D. C. Langreth, and B. I. Lundqvist, Phys. Rev. Lett. **92**, 246401 (2004).
[32]J. P. Perdew, K. Burke, and M. Ernzerhof, Phys. Rev. Lett. **77**, 3865 (1996).
[33]Y. Zhang and W. Yang, Phys. Rev. Lett. **80**, 890 (1998).
[34]P. Giannozzi *et al.*, J. Phys.: Condens. Matter **21**, 395502 (2009); http://www.quantum-espresso.org
[35]H. J. Monkhorst and J. D. Pack, Phys. Rev. B **13**, 5188 (1976).
[36]S. Plimpton, J. Comput. Phys. **117**, 1 (1995); http://lammps.sandia.gov
[37]D. W. Brenner, O. A. Shenderova, J. A. Harrison, S. J. Stuart, B. Ni, and S. B. Sinnott, J. Phys.: Condens. Matter **14**, 783 (2002).
[38]S. J. Stuart, A. B. Tutein, and J. A. Harrison, J. Chem. Phys. **112**, 6472 (2000).
[39]L. A. Girifalco, M. Hodak, and R. S. Lee, Phys. Rev. B **62**, 13104 (2000).
[40]Y. Baskin and L. Meyer, Phys. Rev. **100**, 544 (1955).
[41]L. A. Girifalco and R. A. Lad, J. Chem. Phys. **25**, 693 (1956).
[42]L. X. Benedict, N. G. Chopra, M. L. Cohen, A. Zettl, S. G. Louie, and V. H. Crespi, Chem. Phys. Lett. **286**, 490 (1998).
[43]R. Zacharia, H. Ulbricht, and T. Hertel, Phys. Rev. B **69**, 155406 (2004).
[44]S. D. Chakarova-Käck, E. Schröder, B. I. Lundqvist, and D. C. Langreth, Phys. Rev. Lett. **96**, 146107 (2006).
[45]M. Reguzzoni, A. Fasolino, E. Molinari, and M. C. Righi, J. Phys. Chem. C **116**, 21104 (2012).
[46]E. Zaremba and W. Kohn, Phys. Rev. B **13**, 2270 (1976).
[47]A periodic function can be written as a Fourier series in the form $C_i(\mathbf{r}) = \sum_{\mathbf{g}} C_i(\mathbf{g}) e^{i\mathbf{g}\cdot\mathbf{r}}$ where $C_i(\mathbf{g})$ are Fourier coefficients $C_i(\mathbf{g}) = \frac{1}{A}\int_{\text{cell}} C_i(\mathbf{r}) e^{-i\mathbf{g}\cdot\mathbf{r}} d\mathbf{r}$, A is the area of the unit cell, and $\mathbf{g}$ are reciprocal lattice vectors: $\mathbf{g} = n_1\mathbf{b}_1 + n_2\mathbf{b}_2$ with $n_{1,2}$ integers and $\mathbf{b}_{1,2}$ the primitive vectors of the hexagonal reciprocal lattice. In our case $C_i(\mathbf{g}_{0,0}) = 3C_i^{\min} - 2C_i^{\max}$ and the six coefficients $C_i(\mathbf{g}_{n_1,n_2})$ with $n_1,n_2 = 10,01,11,-10,0-1,-1-1$ are identical to Δ_i. By summing the first seven terms in the above Fourier expansion and considering that $\mathbf{g}_{-10} = -\mathbf{g}_{10}$; $\mathbf{g}_{0-1} = -\mathbf{g}_{01}$; $\mathbf{g}_{-1-1} = -\mathbf{g}_{11}$ one arrives at Eq. (2).
[48]Y. Wang, Y. Ye, and K. Wu, Surf. Sci. **600**, 729 (2006).